Cancer Cell
Article

The Cyclin-like Protein Spy1 Regulates Growth and Division Characteristics of the CD133+ Population in Human Glioma

Dorota Lubanska,[1] Brenna A. Market-Velker,[1] Ana C. deCarvalho,[2] Tom Mikkelsen,[2] Elizabeth Fidalgo da Silva,[1] and Lisa A. Porter[1,*]
[1]Department of Biological Sciences, University of Windsor Ontario, Windsor, ON N9B 3P4, Canada
[2]Department of Neurosurgery, Henry Ford Hospital, Detroit, MI 48202, USA
*Correspondence: lporter@uwindsor.ca
http://dx.doi.org/10.1016/j.ccr.2013.12.006

SUMMARY

The heterogeneity of brain cancers, as most solid tumors, complicates diagnosis and treatment. Identifying and targeting populations of cells driving tumorigenesis is a top priority for the cancer biology field. This is not a trivial task; considerable variance exists in the driving mutations, identifying markers, and evolutionary pressures influencing initiating cells in different individual tumors. Despite this, the ability to self-renew and differentiate must be conserved to reseed a heterogeneous tumor mass. Focusing on one example of a tumor-initiating cell population, we demonstrate that the atypical cyclin-like protein Spy1 plays a role in balancing the division properties of glioma cells with stemness properties. This mechanistic insight may provide new opportunities for therapeutic intervention of brain cancer.

INTRODUCTION

Primary brain tumors can be driven by a population of brain tumor-derived cells with stem-like characteristics or brain tumor-initiating cells (BTICs) (Hemmati et al., 2003; Singh et al., 2004). Whether these cells arise through dedifferentiation of lineage-specified progenitors or through malignant transformation of endogenous neural stem cells (NSCs) is a subject of much debate. Regardless of the origin, understanding how BTICs regulate growth and development is of utmost importance for future treatment strategies (Dean et al., 2005). One commonality among BTICs is that they possess stem cell properties and, analogous to the hematopoietic system, express markers characteristic of primitive neural cells (Chen et al., 2010; Hemmati et al., 2003). Understanding the mechanisms regulating NSC decisions may reveal key mediators dictating the initiation and continued growth of BTICs.

The development of the mammalian brain depends on symmetric division of the NSC population to expand the pool of proliferating stem cells, followed by a switch to asymmetric division to generate the neurons and glial cells in the brain, while maintaining the NSC population (Götz and Huttner, 2005). Cell-cycle regulation appears to underlie the transition between expansion of progenitor pools and differentiation decisions (Dehay and Kennedy, 2007). Lengthening the cell cycle in vitro by inhibiting the cyclin-dependent kinases (CDKs) induces premature generation of neurons (Calegari and Huttner, 2003). Alternately driving the cell cycle by overexpressing CDKs or G1/S cyclins leads to the expansion of neural progenitor cells in the mouse brain (Artegiani et al., 2012; Lange et al., 2009). Stimulating neuronal differentiation in cell culture downregulates endogenous levels and activity of the G1/S CDK, CDK2, as well as increasing protein levels of the CDK inhibitor $p27^{Kip1}$ (p27) (Dobashi et al., 2000; Kranenburg et al., 1995). *CDK2* knockout mice have marked defects in the proliferative capabilities and self-renewal of adult neural progenitors in the subventricular zone (SVZ) (Jablonska et al., 2007). Indeed, enhanced CDK2 activity and downregulation of p27 are observed in many cases of brain cancer (Fiano et al., 2003; Hemmati et al., 2003; Narita et al., 2002). CDK inhibitors have shown efficacy in human glioma in vitro (Jane et al., 2006); however, many biological questions remain to be elucidated before this approach can be reliably used in vivo. Intriguingly, the BTIC

Significance

Brain tumor-initiating cells represent a highly tumorigenic subpopulation within the tumor mass. Resistance to radio- and/or chemotherapy makes this subpopulation a challenge in advancing medicine. Resolving the mechanism driving the expansion of this specific group of cells requires a complete understanding of cell division and differentiation processes occurring in normal neural stem cells. Our data provide insight into how one population of neural cells with stem/progenitor properties relies on a specific cell-cycle regulator to coordinate the fine balance of fate decisions.

population correlates with high levels of positive cell-cycle regulators and reduced levels of cell-cycle inhibitors (Hidaka et al., 2009). Understanding the roles of the core cell-cycle machinery in BTIC expansion has important implications in the treatment of brain cancers.

CDK activity is regulated by the relative abundance of its cyclin-binding partner. More recently, a highly conserved family of ''cyclin-like'' proteins, called the Speedy/RINGO family, has emerged that is regulated developmentally and in a tissue-specific manner (Cheng et al., 2005b). The originally characterized member, Spy1A1 (herein referred to as Spy1), is found at elevated levels in several cancers (Al Sorkhy et al., 2012; Golipour et al., 2008; Porter et al., 2002; Zhang et al., 2012). Spy1 can directly bind and activate the CDKs independent of phosphorylation within the T-loop of the CDK and with decreased dependency on dephosphorylation by the Cdc25 phosphatases (Cheng et al., 2005a). This manner of activating CDKs implies a mechanism by which Spy1 can bypass classically defined cell-cycle checkpoints. Indeed, Spy1 is required for cell-cycle re-entry in maturing vertebrate oocytes (Arumugam et al., 2012; Lenormand et al., 1999). The Spy1 gene, *SPDYA*, was initially isolated as a gene that conferred resistance to UV damage in a *RAD1*-deficient strain of *Schizosaccharomyces pombe* (Lenormand et al., 1999). Since this time, Spy1 protein has been shown to override a number of cell-cycle checkpoints and is capable of directly binding and promoting degradation of p27 (McAndrew et al., 2007; Porter et al., 2003).The implication of this in the molecular processes regulating development and aging is also interesting. In mammary progenitor cells, Spy1 levels are tightly regulated through normal development and accumulated protein levels abrogate differentiation and promote precocious development (Golipour et al., 2008). In the acute sciatic injury model, Spy1 levels are dramatically upregulated in populations of proliferating astrocytes and microglia of the lumbar spinal cord, consequently implicating Spy1 in the regenerative processes of this system (Huang et al., 2009). Interestingly, upregulation of Spy1 is accompanied by an increase in CDK2 activity and downregulation of p27 in this system. Recently, Zhang et al. (2012) demonstrated that Spy1 levels are elevated in malignant human glioma and the protein levels correlate with poor prognosis. The objective of this work was to determine the role of Spy1-directed CDK activity in human glioma.

RESULTS

Spy1 Protein Levels Are Elevated in Multiple Types of Glioma and Correlate with Increasing Tumor Grade

Analysis of the protein levels of Spy1 in oligoastrocytoma (OAC; Figure 1A), oligodendroglioma (ODG; Figure 1B), and invasive glioblastoma multiforme (GBM; stage IV astrocytoma; Figure 1C) was conducted using tissues obtained from the Ontario Brain Tumor Tissue Bank. Each sample set analyzed consisted of tissue derived from the tumor center (I), peritumor (II-IV), and normal tissue (V). Average levels of Spy1 protein from tumor center out to normal tissue were calculated over three sets of samples per patient (Figures S1A–S1C available online). Spy1 protein levels were significantly elevated in the tumor tissue over normal in 3 of 4 OAC and ODG sample sets and 1 of 4 GBM sample sets (Figure S1A–S1C). Notably, tumor samples from patients 865 (OAC; Figure 1A), 976, and 977 (GBM; Figure 1C) were noted as being highly necrotic in patient records, and Spy1 levels were not elevated in these samples. In all 32 sample sets, combined Spy1 protein levels were significantly elevated in 63% of samples from the tumor center and 62% of peritumor samples in comparison to the pair matched control tissues.

To further correlate the levels of Spy1 protein with the grade of brain tumor, we utilized tissue microarrays (TMAs) consisting of 188 different patient cores, including cores taken from noncancerous (normal) brain samples. Representative hematoxylin and eosin-stained core images are presented in Figure S1H. Immunohistochemistry (IHC) performed on TMAs revealed extensive Spy1 staining in tumor tissues over pair-matched adjacent normal brain tissues taken from the same patients (Figure 1D; Figure S1I). Spy1 protein levels were progressively elevated with increasing grade of astrocytoma, demonstrating statistical significance over benign tissue as well as both pair match normal adjacent tissue and noncancerous normal tissues (combined as ''normal'') (Figure 1E). Although sample numbers were limited, we found that Spy1 levels correlated with increasing grade of OAC (Figure S1D) and ODG (Figure S1E). Overall, protein levels of Spy1 were elevated at least 2-fold in 69% of the glioma tumor samples (Figures 1A–1E; Figures S1D and S1E). Work performed by The Cancer Genome Atlas (TCGA) research network demonstrated a strong correlation between the established GBM classes and normal neural lineages (Verhaak et al., 2010). Notably, we found that in comparison to primary neural cells cultured in monolayer, Spy1 expression levels are significantly upregulated in neurospheres derived from clonal expansion of those cells and correlate with the expression of stemness markers, such as Nestin and Vimentin (Figure S1G).

Amplification of the *SPDYA* Locus Correlates with Poor Patient Prognosis

To determine if alterations at the genetic locus of Spy1 could be implicated in patient prognosis, survival data from the Rembrandt NCI database were used to evaluate the effects of Spy1 and the Spy1 effector CDK2 on overall patient survival (NCI, 2005). CDK2 was found to be overexpressed in 236 out of 343 cases of all glioma, and overexpression very significantly correlated with reduced patient survival, $p < 0.001$ (Figure 1F). Importantly, there were no cases of downregulation of CDK2 in all 343 cases. Similarly, in the data set of Li et al. (2009a) consisting of 257 patients, there were 198 cases with upregulated CDK2, no cases of significant downregulation, and upregulation very significantly correlated with decreased survival, $p < 0.001$ (data not shown). *SPDYA* was found to be amplified in 31 of 56 cases of ODG, and amplification statistically correlated with reduced patient survival, $p = 0.01$ (Figure S1F). *SPDYA* was amplified in 3 of 5 cases of mixed glioma, and amplification correlated with reduced patient survival, $p = 0.06$ (data not shown). For total glioma cases, *SPDYA* was amplified in 143 out of 222 cases of all glioma, and amplification significantly correlated with reduced patient survival, $p = 0.005$ (Figure 1G). Notably, the Rembrandt database does not specify whether locus amplification is due to events such as focal

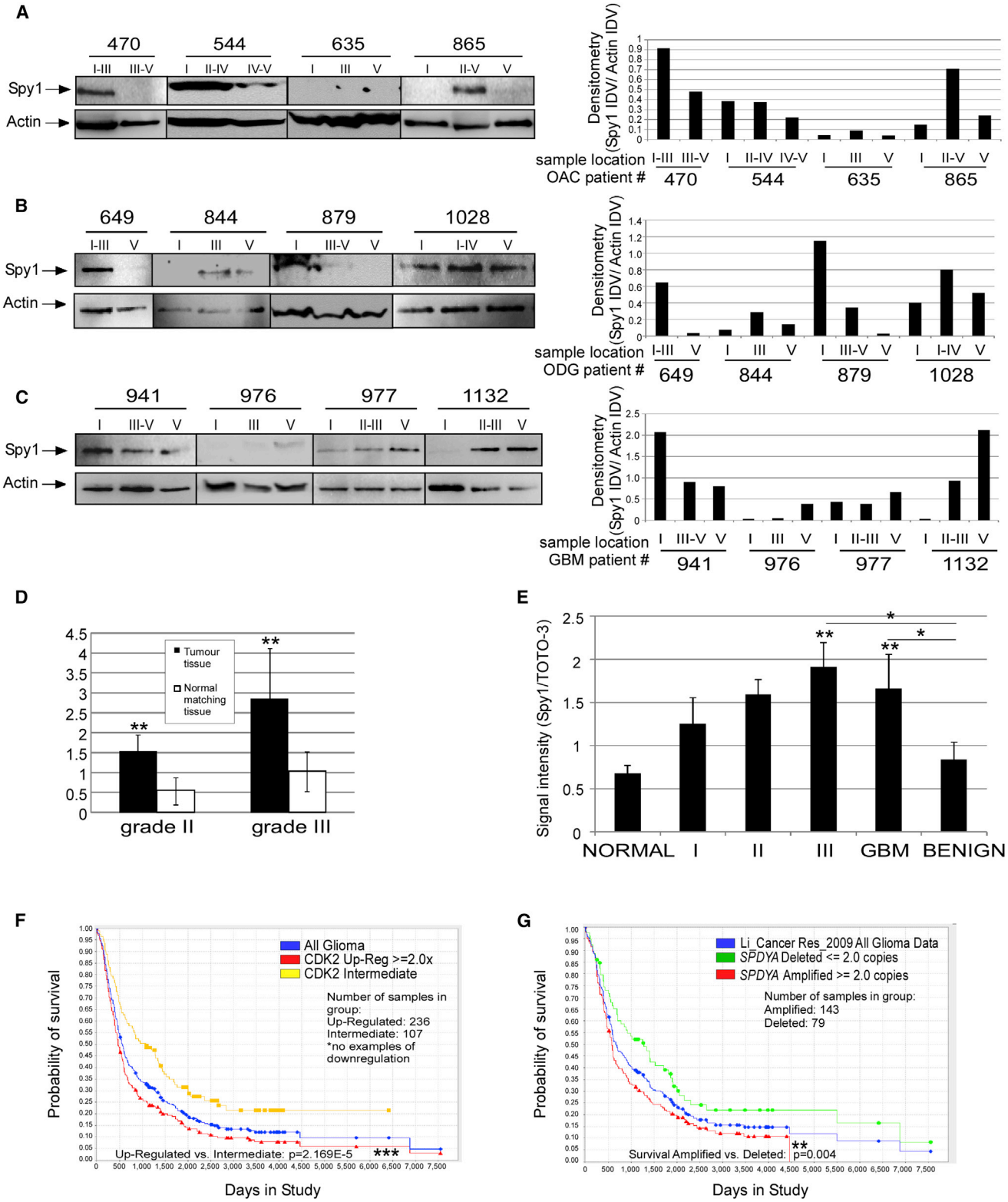

Figure 1. Spy1 Protein Is Overexpressed in High-Grade Glioma

(A–C) Spy1 protein expression in human brain tumor tissues microdissected from OAC (A), ODG (B), and GBM (C) patients. Biopsies were taken from the tumor center (I), peritumor (near tumor infiltrate-scant tumor cells [II–IV]), or normal brain tissue (V). Patient identifier number is noted in each panel. One representative blot of three is depicted. Values presented as the mean of integrated density values (IDV) Spy1/Actin. Average values over three blots of the same sample set are quantified in Figures S1A–S1C.

(legend continued on next page)

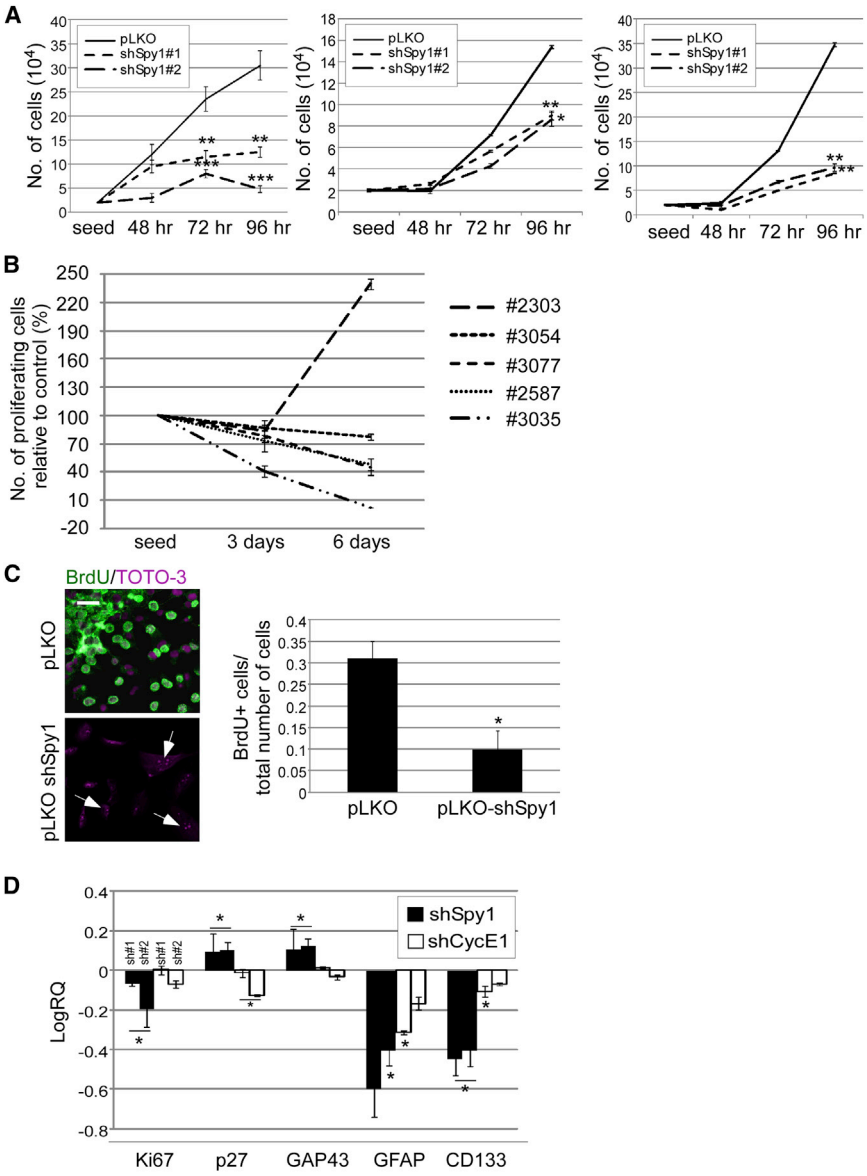

Figure 2. Spy1 Levels Are Essential for Proliferation and Stem-like Properties of Human Glioma Cells

(A) Growth curves measured by trypan blue exclusion for U87 (left), SJ-GBM2 (middle), and U251 (right). See Figure S2A.

(B) Growth curves measured by trypan blue exclusion for human primary brain tumor cells (patient identifier numbers: 2303, 3054, 3077, 2587, and 3035) presented as a percentage of proliferating cells relative to control at the indicated time points. See Figure S2B.

(C) Imaging (left panel) and quantification (right panel) of U87 cells positive for BrdU staining. Data are shown as mean ± SD. At least five fields of view per infection. Scale bar, 10 μm.

(D) qRT-PCR of U87 cells infected with scrambled control (pLKO) or two different shRNA against Spy1 (black bars) or CycE1 (hollow bars). Genes indicated on x axis. See Figures S2C and S2D.

All data are shown as mean ± SD; *$p < 0.05$, **$p < 0.01$, ***$p < 0.001$. n = 3 for each panel. All p values are based on analysis control versus treatment.

amplification or whole arm gain. Nonetheless, from these data, amplification of *SPDYA* and overexpression of the Spy1 effector, CDK2, significantly correlate with reduced survival in glioma patients.

Knockdown of Spy1 Reduces Proliferation and Stemness Properties in Human Glioma

To address the importance of Spy1 in brain tumorigenesis in vitro, we utilized the human U-87MG (U87), SJ-GBM2, and U251 glioma cell lines, as well as primary cells obtained from six consenting patients. The heterogeneous U87 and U251 lines are driven by a well-characterized pool of highly tumorigenic cells that stain positive for the cell-surface marker CD133 ($CD133^+$) (Jin et al., 2011; Kelly et al., 2010). The SJ-GBM2 cells are established from an aggressive pediatric glioma and also possess a significant $CD133^+$ population (Donovan et al., 2012; Middlemas et al., 2000). Cells were infected with lentivirus carrying two different small hairpin RNA (shRNA) constructs against Spy1 (shSpy1) or a scrambled control (pLKO) and were subsequently selected. Both of the Spy1-shRNA constructs effectively reduced their targeted genes at least 3-fold (Figure S2A). Proliferation kinetics show that Spy1-knockdown (KD) significantly reduces cell growth in all cell lines tested (Figure 2A) and in 4 out of 5 primary lines (Figures 2B and S2B). In the -primary tumor cells, the effect of Spy1-KD was rescued by overexpression of a human Spy1 plasmid resistant to knockdown with Spy1-shRNA (pEIZ-Rescue); this confirms target specificity (Figure S2B). Results were confirmed by BrdU incorporation in the U87 line, where the shSpy1 cells showed

(D and E) TMAs containing normal brain and diverse brain tumor tissue samples stained for Spy1 expression. The Spy1 signal intensity is normalized to nuclear stain (TOTO-3) signal. See Figures S1H and S1I. (D) IHC of Spy1-positive cells in astrocytoma tissues of different grade (black bars) in comparison to normal adjacent brain tissue (white bars) over two separate arrays. Grade I–II astrocytoma (n = 3), grade III astrocytoma (n = 3), and normal controls (n = 6). See Figures S1D and S1E.

(E) Spy1 protein levels analyzed in different grades of astrocytoma (I–III) (n = 112), GBM (n = 24), benign brain tumors (n = 8), and normal controls (n = 19).

(F and G) Patient survival data from Rembrandt NCI database correlated with CDK2 expression levels over all glioma samples (F) or *SPDYA* amplification/deletion from all glioma data (G). See Figure S1F.

All data are shown as mean ± SD; *$p < 0.05$, **$p < 0.01$, ***$p < 0.001$.

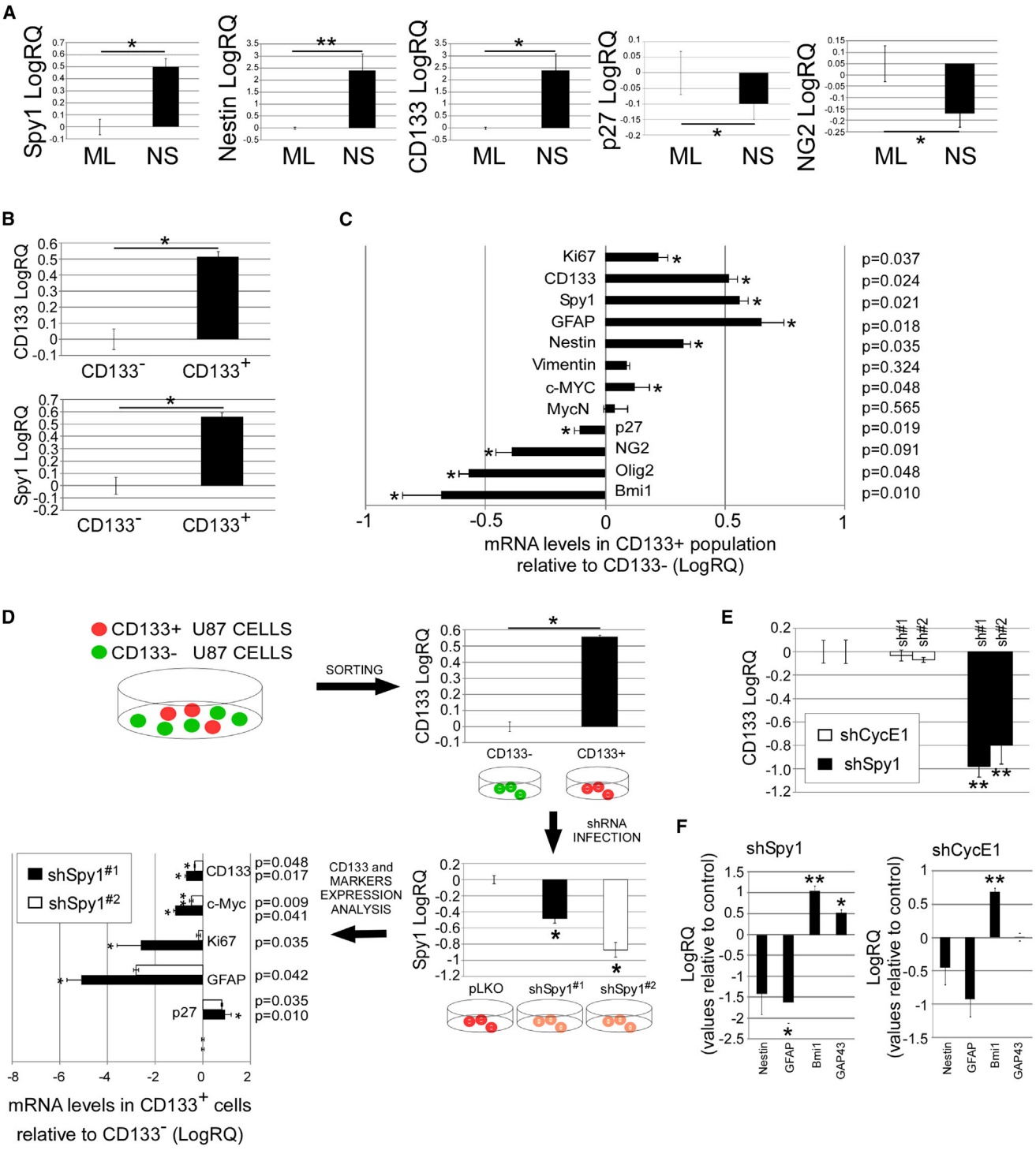

Figure 3. Spy1 Expression Plays a Critical Role in the Stemness Properties of the CD133$^+$ BTIC Population

(A) qRT-PCR of U87 cells cultured as monolayer (ML) or in a neurosphere formation assay (NS) at passage 5.

(B) U87 cells sorted and CD133$^+$ and CD133$^-$ populations analyzed by qRT-PCR for CD133 (upper panel) and Spy1 (lower panel) levels.

(C) CD133$^+$ and CD133$^-$ populations analyzed by qRT-PCR for several genes. The CD133$^+$ population is compared to the CD133$^-$ population. p values are presented.

(D) U87 cells sorted for CD133 (confirmed by qRT, top right graph). The CD133$^+$ population was infected with either shRNA control (pLKO) or one of two shSpy1 constructs (shSpy1$^{\#1}$ [solid bars] or shSpy1$^{\#2}$ [hollow bars]). Knockdown confirmed by qRT-PCR (lower right graph). Effects on gene expression reported as relative expression of shSpy1over pLKO control (lower left graph). p values are presented.

(legend continued on next page)

over a 60% reduction in DNA synthesis compared to control cells (Figure 2C).

Marker analysis in three different human primary cell lines determined that collectively Spy1-KD caused significant downregulation of CD133, downregulation of Nestin, and significant upregulation of β-III Tubulin levels (Figure S2C). Spy1-KD in U87 cells significantly reduced expression of the proliferation marker Ki67 and enhanced expression of p27 (Figure 2D). Interestingly, Spy1-KD also correlated with increased levels of the growth-associated protein 43 (GAP43), a marker of mature neurons, and decreased levels of markers known to identify normal stem-like cells and BTICs, CD133, and glial fibrillary acidic protein (GFAP). These data prompted the hypothesis that Spy1 levels may be important for both proliferation and directing the fate of at least subsets of cells within the heterogeneous tumor.

Spy1 binds and activates CDK2 in a manner distinct from that of classical cyclin proteins, and Spy1-bound CDK2 has altered substrate specificity when compared to Cyclin E/A-bound CDK2 (Cheng et al., 2005a). Hence, to determine if Spy1 has unique roles in proliferation and stemness in human glioma, we compared Spy1-KD effects to reduced expression of Cyclin E1 (CycE1) in a heterogeneous population of U87 cells. Here, we targeted CycE1 using two different shRNA constructs (Figure S2D). We found that there were some similarities in response, where both Spy1-KD and CycE1-KD reduced expression of the stemness markers GFAP and CD133 (Figure 2D). However, there were also some pronounced differences; CycE1-KD did not have a significant effect on the proliferation marker Ki67 and had an opposite effect on both p27 and the neuronal differentiation marker GAP43.

Spy1 Regulates Stemness Properties of the CD133$^+$ Glioma Population

To determine the potential role of Spy1 in the BTIC populations with neurosphere formation capacity, U87 cells were cultured and passaged in monolayer or as spheres to promote self-renewal in vitro (Lee et al., 2006). Spy1 expression levels were upregulated when cells were cultured as spheres (Figure 3A). This increase correlated with upregulation of the stemness markers Nestin and CD133 and downregulation of p27 and the oligodendrocyte marker NG2 (Figure 3A). CD133-negative (CD133$^-$) cells are capable of initiating tumors in vivo; however, sorting for a CD133$^+$ population in human glioma has been shown to enrich sphere formation, initiate glioma in a mouse xenograft model, and to correlate with decreased prognosis for glioma patients (Bao et al., 2006; Zeppernick et al., 2008). Spy1 expression is significantly higher in the CD133$^+$ population, and this correlates positively with expression of the stem/progenitor markers Nestin and Vimentin (Figures 3B and 3C). This population also expressed higher amounts of the proliferation marker Ki67 along with the oncogenes c-Myc and MycN and reduced expression of p27 (Figure 3C). Additionally, the CD133$^+$ population was characterized by lower expression of oligodendrocyte markers Olig2 and NG2, which, along with the upregulated levels of GFAP, suggests an astrocyte progenitor lineage and supports NSC nature of these cells. Downregulation of Bmi1 suggested that the sorted population represents a higher stem-like hierarchy, as Bmi1 was recently shown to mark progenitor populations at the intermediate stages of differentiation within human glioma (Venugopal et al., 2012).

We then measured the effects of depleting Spy1 on stemness characteristics of the CD133$^+$ population in multiple established cell lines. In U87 cells sorted for CD133 (Figure 3D, top panel), Spy1-KD resulted in a marked reduction of CD133 levels that occurred along with a decline in BTIC/proliferation markers GFAP, Ki67, c-Myc, and upregulation of p27 levels (Figure 3D, bottom left panel). These results were similar in other glioma cell lines known to contain a CD133$^+$ population (Figures S3A and S3B). Notably, the c-Myc, Ki67, and p27 effects were not assessed for significance in the U251 cells (Figure S3B). Although both shRNA constructs consistently reduced CycE1 expression at least 14-fold in the sorted population (Figure S3C) and significantly reduced kinase activity as compared to Spy1-KD (Figure S3D), there were no significant effects on the expression of the BTIC marker CD133 (Figure 3E). Furthermore, only Spy1-KD demonstrated a significant effect on reducing the stemness markers Nestin and GFAP and increasing expression of neuronal markers, such as GAP43, in the CD133$^+$ population (Figure 3F). Interestingly, KD of both Spy1 and CycE1 resulted in an increase in Bmi1. It has recently been demonstrated that, whereas Bmi1 drives NSC self-renewal, expression tends to mark a population of cells that is more differentiated than the CD133$^+$ (Venugopal et al., 2012). Collectively, these results support the conclusion that inhibition of CDK2 activity begins to transition the CD133$^+$ population to a more differentiated state, but CycE1-KD alone is not sufficient to denote changes in stemness or more differentiated markers.

Downregulation of Spy1 Is Critical for Specific Differentiation Decisions

Given that Spy1-KD reduced expression of stem/progenitor markers and increased neuronal differentiation markers, we questioned whether Spy1 was endogenously regulated during differentiation. The SVZ region of postnatal mouse brains were microdissected at days 1–4 and grown as monolayer (Figure 4A) or neurospheres (Figure S4A), followed by treatment with differentiation stimuli. In both cases, Spy1 expression decreased with differentiation morphology and correlated with a decrease in stemness markers GFAP and Nestin and an increase in the neuronal differentiation marker GAP43 (Figures 4A and S4A). To determine whether decreasing levels of Spy1 protein are essential for differentiation to occur, Spy1 or an empty vector control were overexpressed in primary neural cells (Figure 4B). We found that 60% of control spheres successfully differentiated by 72 hr, whereas only ~20% of Spy1-overexpressing neurospheres were visibly differentiating (Figure 4B). Spy1-overexpressing cells, induced to differentiate, had reduced expression

(E) qRT-PCR for CD133$^+$ cells infected with shSpy1, shCycE1, or scrambled sh-Control (pLKO). Representative data are shown.
(F) qRT-PCR of different markers (x axis) from the CD133$^+$ population treated in part (E) above. Left panel reflects Spy1-KD, and the right panel reflects CycE1-KD; values are averaged over two separate shRNA constructs each ran in triplicate over three individual experiments.
All data are shown as mean ± SD; *$p < 0.05$, **$p < 0.01$, ***$p < 0.001$. Unless indicated, n = 3. See also Figure S3.

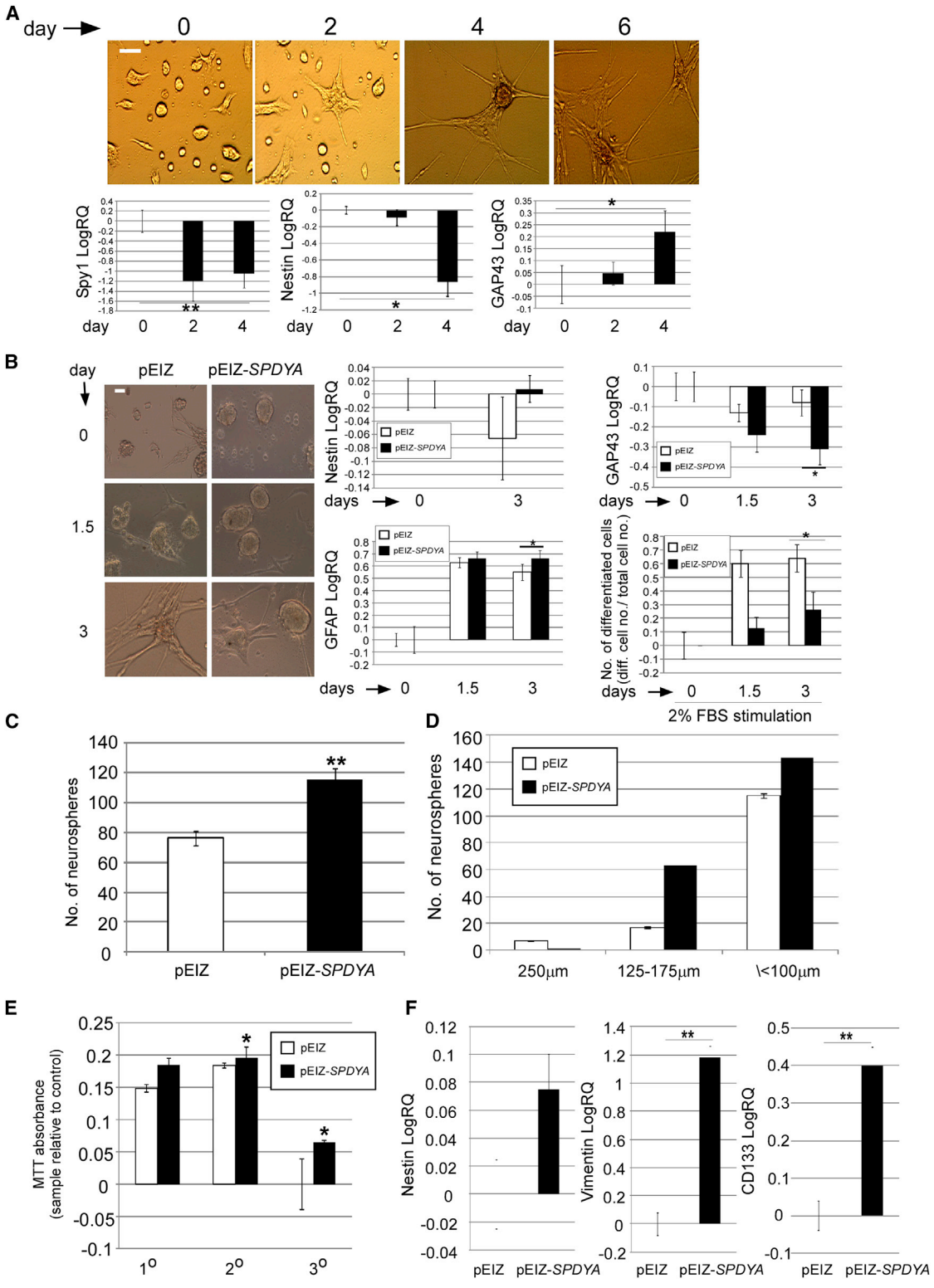

Figure 4. Spy1 Overexpression Abrogates Neuronal Differentiation and Promotes Neurosphere Clonal Growth

(A) Differentiation of mouse primary neural cells recorded by phase contrast microscopy (upper panels; scale bar, 10 μm). qRT-PCR of Spy1, GAP43, and Nestin tested along the differentiation time course (lower panel). Nontreated cells were used as a control.

(B) Primary neurospheres infected with pEIZ-*SPDYA* versus empty vector control (pEIZ) over the indicated time points. Morphology was monitored by light microscopy (upper left panel). Scale bar, 25 μm. Differentiation was scored by neurite length and presented as the ratio of differentiated spheres to total spheres

(legend continued on next page)

of the neuronal differentiation marker GAP43 and enhanced expression of the progenitor marker GFAP (Figure 4B). Although levels of Nestin were increased, they were not significant (Figure 4B). Effects on mature astrocytes require further investigation pending the expansion of available markers. Depletion of Spy1 in primary neural cells using shRNA demonstrated a significant increase in functional differentiation; these effects were rescued using the Spy1 rescue (pEIZ-Rescue) construct (Figure S4C). These results support that elevated levels of Spy1 favor expansion of stem/progenitor cells possessing glial characteristics and prevent functional differentiation toward a neuronal lineage.

To further determine whether Spy1 levels are critical for normal stem/progenitor characteristics, primary neural cells manipulated for Spy1 or control were assessed using established assays to measure self-renewal capacity and neurosphere formation (Guryanova et al., 2011; Lathia et al., 2010). Spy1-overexpressing cells significantly increased the overall number, clonality, and viability of neurospheres as compared to controls (Figures 4C–4E). An opposite effect was observed with Spy1-KD (Figure S4B). Cells overexpressing Spy1 had notable elevation in the expression of stemness markers, such as Nestin, Vimentin, and CD133 (Figure 4F). These data demonstrate that the cyclin-like protein Spy1 is an important regulator in the expansion and growth of NSCs. Although these data do not reveal a cell of origin, we provide an additional mechanistic link regulating the common growth characteristics between neural stem/progenitor cells and BTIC populations.

Symmetric Division of CD133$^+$ U87 Glioma Cells Relies on Spy1

To assess the effects of Spy1 on the self-renewal characteristics of BTICs in human glioma, cell lines, or primary brain tumor cells with manipulated levels, either Spy1 or CycE1 were cultured at low densities (<10 cells/well) in media supporting self-renewal. Sphere formation was measured over 28 days after plating, and spheres of 25 μm or more in diameter were scored (Figures 5A–5C). In the established cell lines, as well as in 3 out of 5 primary lines tested, Spy1-KD caused significant reduction in both the number (Figures 5A–5C) and diameter (Figures 5B and 5C) of resulting spheres; these are characteristics previously correlated with tumorigenic capacity and percent of CD133$^+$/Nestin$^+$ cells in glioma (Wang et al., 2008; Yoon et al., 2012). In primary cells, the effect was significantly rescued, utilizing the Spy1 pEIZ-Rescue construct altered to confer resistance to shRNA used (Figure 5A). Sphere formation over an excess of ten passages in CD133$^+$ U87 cells revealed that Spy1-KD caused a 5-fold decrease in number and longevity of spheres compared to control (Figures S5A, left panel, and S5B). The reciprocal effect was also noted in cells overexpressing Spy1 (pEIZ-*SPDYA*; Figure S5A, right panel). EGF and FGF are essential growth factors that support stem cell self-renewal (Li et al., 2009b; Reynolds and Weiss, 1992). Interestingly, Spy1 overexpression resulted in a significant increase in CD133$^+$ cells in the absence of EGF/FGF (Figure S5C). This supports the hypothesis that cell-cycle regulation by Spy1 may lie downstream of associated growth factor signaling.

How BTICs use symmetric versus asymmetric division to regulate expansion and support tumor growth is a very important point not fully understood. Utilizing computer modeling, Boman et al. (2007) have established that increasing symmetric division is the only mechanism to adequately explain the expansion of the cancer stem cell population. *Drosophila* and mammalian systems have shown that symmetry of division is influenced by the segregation of the protein Numb (Knoblich et al., 1995; Lu et al., 1998). Numb is able to promote neural differentiation, at least in part, through antagonizing Notch and Hedgehog pathways; thus, localization of Numb serves as an indicator of cellular fate determination (Couturier et al., 2012; Di Marcotullio et al., 2006). Although the functional role is unknown, we do know that asymmetric distribution of CD133 also colocalizes with Numb in differentiating glioma stem cells (Lathia et al., 2011). Utilizing the cell pair assay to monitor protein expression in single cells through division, we found that Spy1-KD resulted in marked asymmetric distribution of both Numb (Figure 5D; Figures S5D and S5E) and CD133 protein (Figure 5D). Analysis over multiple infections of multiple glioma cell lines with two separate knockdown constructs for CycE1 and Spy1 showed significant asymmetric localization of Numb protein in the Spy1-KD cells, but not in the CycE1-KD cells (Figure 5D). The mode of division analysis utilizing human primary brain tumor cells revealed the same result, that the depletion of Spy1, but not of CycE1, levels resulted in a significant increase in the number of cells dividing asymmetrically as determined by Numb distribution (Figure 5E). Spy1-KD effects were significantly reversed by the Spy1 pEIZ-Rescue construct. Interestingly, Spy1-KD effects were also reversed by the overexpression of CycE1, and effects were mimicked by the CDK2 inhibitor, NU2058. These data support the conclusion that activation of CDK2 toward noncanonical substrates that are preferred by Spy1-directed CDK activity (Cheng et al., 2005a), but can also be activated by gross CDK activation, regulates symmetric division in glioma stem cells. Western blot analysis of Numb protein expression levels in CD133$^+$ cells upon Spy1-KD or CycE1-KD show that Spy1 downregulation, but not downregulation of CycE1, causes a significant and repeatable accumulation of Numb protein levels (Figure 5F). Interestingly, even within heterogeneous populations of human glioma, Spy1 levels were found to inversely correlate with Numb and p21 levels (Figure S5F). Collectively, these data support the

(lower left panel). Control (hollow), Spy1 overexpressing (black bars). qRT-PCR of markers in control (pEIZ) and Spy1-overexpressing (pEIZ-*SPDYA*) primary cells (right panel top to bottom).

(C) Clonal assay performed on primary neural cells overexpressing Spy1 (pEIZ-*SPDYA*) versus control (pEIZ). Total neurosphere numbers indicated.

(D) Neurospheres scored according to diameter after they were maintained in culture for 14–20 days. n = 2.

(E) Longevity of pEIZ or pEIZ-*SPDYA* primary, secondary, and tertiary neurospheres (NS) in culture assessed by MTT assay. Neurospheres were passaged as single cells every 6–9 days. Absorbance at 590 nm corrected for background absorbance.

(F) qRT-PCR of stemness markers in pEIZ or pEIZ-*SPDYA* primary cells cultured as neurospheres (NS).

Unless indicated, data are shown as mean ± SD, n = 3. *p < 0.05, **p < 0.01, ***p < 0.001. See also Figure S4.

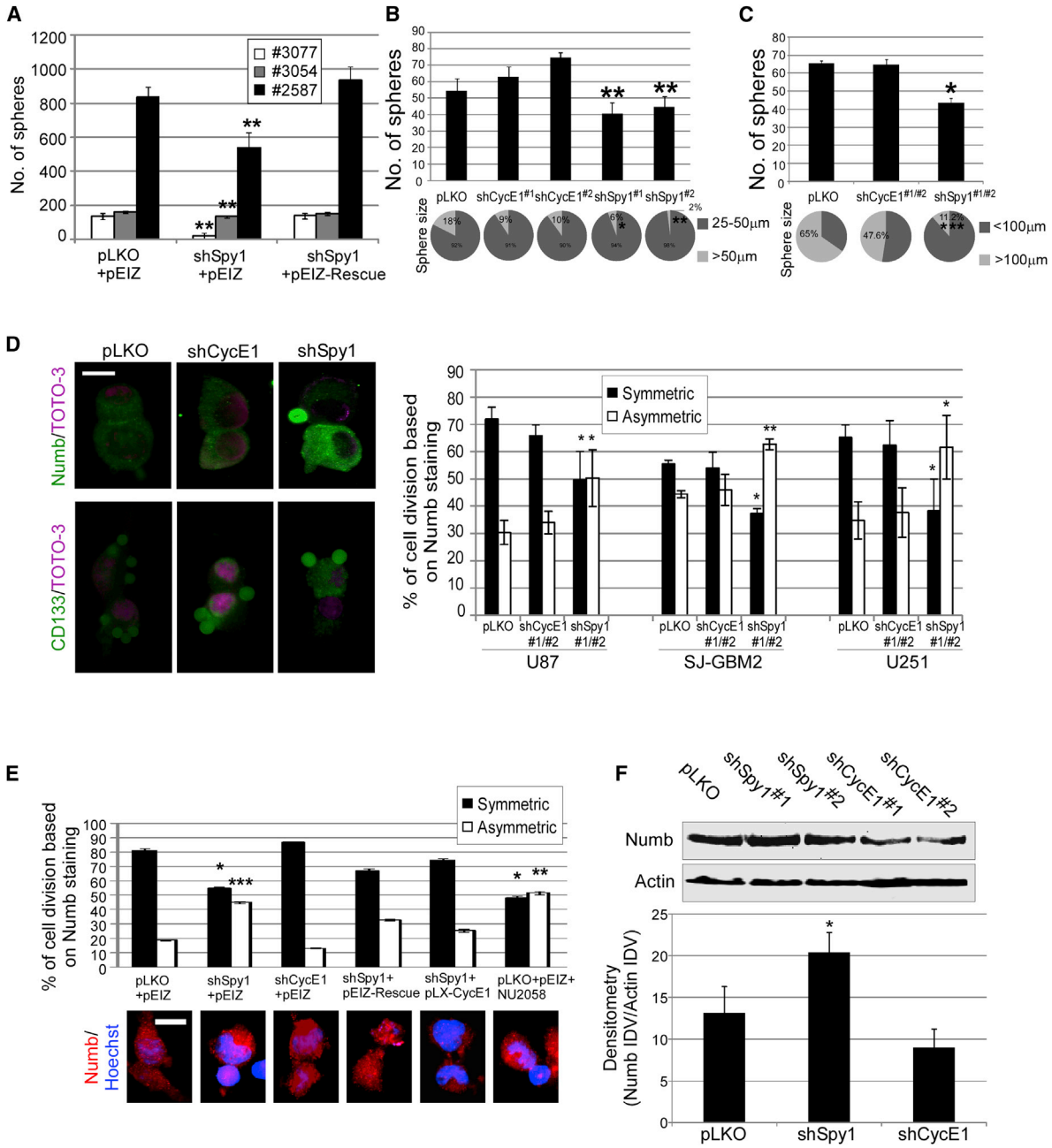

Figure 5. Spy1 Is Critical for Symmetric Division and Self-Renewal of CD133$^+$ Cells

(A) Clonal assay performed on control (pLKO+pEIZ), shSpy1 (shSpy1+pEIZ), and overexpressing rescue vector (shSpy1+pEIZ-Rescue) human primary brain tumor cells. Emerging neurospheres of over 25 μm scored per well. There is a minimum of 30 wells per replicate.

(B and C) As described for (A) using the CD133$^+$-enriched U87 (B) and SJ-GBM2 (C) cells treated with pLKO-Control (pLKO), shSpy1$^{\#1/\#2}$, and shCycE1$^{\#1/\#2}$. Neurosphere size is presented as a pie chart. Results obtained from both shRNA constructs were pooled for (C). See Figures S5A–S5C.

(D) Cell pair assay conducted using the CD133$^+$ population of U87, SJ-GBM2, and U251 cells treated with pLKO-Control (pLKO), shSpy1$^{\#1/\#2}$, and shCycE1$^{\#1/\#2}$. Representative U87 cells stained for Numb (left upper panel) and CD133 (left lower panel). Quantification of each cell type scored for Numb distribution (right panel). Scale bars, 10 μm. See Figures S5D and S5E.

(E) Cell pair assay conducted using human primary brain tumor cells treated as above, as well as with shCycE1 (shCycE1+pEIZ), CycE1-overexpressing vector alone (pLX-CycE1), or together with shSpy1 (shSpy1+pLX-CycE1), CDK2 inhibitor (pLKO+pEIZ+NU2058), and Spy1 rescue vector alone (pLKO-pEIZ-Rescue). Quantification of each cell type was scored for Numb distribution (top panel). Representative cells were stained for Numb (red) and nuclei (blue) (bottom panel). Scale bar, 10 μm.

(F) Levels of Numb protein in U87 cells treated with shSpy1 or shCycE1. One representative blot of three (upper panel).Values are presented as the mean of integrated density values (IDV) Numb/Actin. See Figure S5F.

Unless indicated, data are shown as mean ± SD, n = 3. *p < 0.05, **p < 0.01, ***p < 0.001.

conclusion that endogenous levels of the atypical cyclin-like protein Spy1 promote NSC self-renewal and expansion of stem/progenitor populations by regulating the balance of symmetric versus asymmetric division.

DISCUSSION

The dynamics of neurogenesis relies on the balance of stem/progenitor self-renewal with commitment to specific lineages. Extensive literature indicates that antiproliferative genes preventing the activation of G1/S CDKs act as important timers to permit neurogenesis (Durand et al., 1998; Hindley and Philpott, 2012). Similarly, although not as extensively investigated, proliferative genes and signals resulting in an activation of the G1/S CDKs support expansion of stem/proliferative populations and retard successful neurogenesis (Dobashi et al., 1995; Lange and Calegari, 2010). Which cyclin-CDKs regulate specific neurogenic events and how their activation is controlled remain to be elucidated. As multicellular organisms have evolved to possess regenerative systems capable of sustaining long life, so have the families of proteins regulating cell-cycle progression. The Speedy/RINGO family of cyclin-like proteins is such an example. Expressed in all vertebrates and some invertebrates, at least one family member, Spy1, has demonstrated roles in spinal cord regeneration and to possess stem-like qualities in the developing mammary gland (Golipour et al., 2008; Huang et al., 2009). In this work, we demonstrate that Spy1 is expressed at high levels in clonally derived neurospheres and that levels decline during differentiation. Elevated levels of Spy1 prevent functional differentiation and enhance the number and longevity of neural stem/progenitor cells able to grow in neurosphere culture. Although the link between NSCs and BTICs remains to be determined, BTICs are found to express several normal NSC markers and possess growth characteristics mimicking that of normal NSCs (Chen et al., 2012). Hence, regardless of the BTIC origin, resolving the regulatory properties driving normal stem/progenitor cells may shed light on potential ways to target these aggressive populations therapeutically.

A defining property of both NSCs and BTICs is the ability to divide both symmetrically and asymmetrically. A shift in division characteristics to favor symmetric division contributes to exponential increase in the numbers of cancer stem cells in different types of tumors (Gönczy, 2008). The critical switch between modes of division correlates with changes in the cellular distribution of the protein Numb (Song and Lu, 2012). Functionally, Numb inhibits the Notch pathway to permit asymmetric division and subsequent differentiation (Song and Lu, 2012). Our study demonstrates that Spy1 is important for maintaining symmetric mode of division and self-renewal, implicating a mechanistic role for this "cyclin-like" protein in retaining the hallmark properties of BTICs. Arumugam et al. (2012) pointed at the Spy1 (referred to as RINGO in this publication)-CDK signaling pathway as a highly conserved activator of Musashi-1 (Msi1) during cell-cycle re-entry in oocyte maturation. Activated mammalian Msi1 stimulates Notch signaling through the translational repression of Numb (Imai et al., 2001). Hence, Msi1 may rely on Spy1-directed CDKs to mediate self-renewal of normal NSCs, as well as clonal expansion, malignancy, and proliferation of glioblastoma cells (Muto et al., 2012; Sakakibara et al., 2002). Our data reveal that Spy1-KD, but not CycE1-KD, leads to increased levels of Numb, followed by altered expression of select Notch transcriptional targets. The altered regulation of Numb, and consequently Notch, may also alter overall self-renewal parameters. Noseda et al. (2004) showed that Notch can act as a transcriptional repressor of p21, which further prevents nuclear localization of Cyclin D-CDK4. In mammals, p21 maintains quiescence of adult NSC populations (Kippin et al., 2005). Hence, Spy1 appears to coordinate signals directing both self-renewal and the balance of symmetric/asymmetric division.

It is known that Spy1 activates CDKs in a Cyclin-Activating Kinase (CAK)-independent manner and demonstrates less stringent substrate specificity than cyclin-bound CDKs (Cheng et al., 2005a). In addition, atypical of cyclins, Spy1 can both activate CDKs and directly bind and promote the degradation of the CDK inhibitor p27 (Porter et al., 2003). Functional differentiation requires a decrease in the kinase activity of CDK2 as well as an accumulation in p27 protein levels (Dobashi et al., 1995; Sasaki et al., 2000). This work supports the specific requirement for this class of proteins over the established CDK2 partners during neural differentiation and in promoting stemness properties in neural cells. The importance of these "cyclin-like" proteins has been overlooked in the cancer therapeutics arena for over a decade (Porter et al., 2002). Although CDK inhibitors are being tested clinically for a number of different types of cancer, the studies in brain malignancies remain preliminary (Fischer and Lane, 2000; Jane et al., 2006). In other types of cancer, despite the preclinical success of this approach, the data on actual therapeutic outcome have been quite disappointing (Stone et al., 2012). Our study adds to the accumulating evidence that will aid in improving the effectiveness of CDK inhibitors in their use as chemotherapeutic agents for specific subsets of cancer.

Determining how to direct treatment to the appropriate patient population is a pressing area of cancer research. Spy1 levels were most significantly elevated in higher grades of glioma, known to be more anaplastic with features resembling immature astrocytes and/or oligodendrocytes. This correlates with the elevated levels of glial progenitor markers seen in our cell systems overexpressing Spy1, such as the BTIC marker CD133. A significant amount of data supports the use of CD133 as a stem cell surface antigen to identify a subpopulation of brain tumor-initiating stem cells (Singh et al., 2004). Whereas $CD133^-$ BTIC populations are able to generate heterogeneous tumors in vivo (Korur et al., 2009), tumors containing a $CD133^+$ BTIC population correlate positively with higher grades of glioma, poorer patient prognosis, and multidrug resistance (Dean et al., 2005; Yan et al., 2011; Zeppernick et al., 2008). Resolving the lineage commitment, stage of differentiation, and genetic/genomic signatures of BTIC populations for the different forms and stages of glioma is an essential next step in correlating prognostic markers with effective treatments for brain cancers. Importantly, Spy1-KD in a heterogeneous population of GBM cells decreased the proliferative index, as well as the expression levels of CD133 and GFAP. Abrogation of normal differentiation events can contribute to the initiation of tumorigenesis, and understanding such events has proven to constitute a valuable strategy in the treatment of acute promyelocytic leukemia

(Sell, 2005). Hence, it is feasible that a similar strategy would be a valuable approach for a cancer of neural origin.

EXPERIMENTAL PROCEDURES

Animals

Balb/c mice (Jackson Laboratory) were maintained and cared for following the regulatory standards identified by the Canadian Council for Animal Care. Approval was provided by the University of Windsor animal care committee (AUPP# 10-08).

Primary Mouse Cell Harvest and Culture

Tissues were microdissected, and primary cells were dissociated from the region surrounding the SVZ of P1-P4 mouse brains as described previously (Pacey et al., 2006). Cells were seeded at less than 5×10^4 cells per well in six-well Ultra-Low Cluster Plates (ULCP) (Corning, 3471) and cultured in serum-free Dulbecco's modified Eagle's medium (DMEM)/Ham's Nutrient Mixture F-12 media (Sigma) containing N2 supplement hEGF (20 ng/ml; GIBCO) and bFGF (10 ng/ml; Sigma), 2 mM L-glutamine at 37°C in 5% CO_2. Formed spheres were subcultured every 5–10 days. Differentiation was conducted on primary spheres in media supplemented with 2% FBS as described previously (Kerosuo et al., 2008). Primary, secondary, and tertiary neurospheres were dissociated, and 10,000 cells were seeded in 100 μl of media in 96-well antiadhesive plates. MTT solution (20 μl of 5 mg/ml in PBS) was added to each well and incubated for 4 hr. Extraction buffer (100 μl) was added for 2 hr to dissolve the formazan crystals, and the absorbance at 590 nm was assessed using Victor plate reader (PerkinElmer). Clonal assays were conducted in neurosphere media in 96-well ULCP plates; cells were plated by serial dilution; and wells containing 1–10 cells/well were included in experiments and analysis.

Cell Lines

Human GBM U-87 MG cells were obtained from the American Type Culture Collection. The U251 cell line was a kind gift from Dr. James Rutka (The Hospital for Sick Children Research Institute, University of Toronto). The SJ-GBM2 cell line was obtained from The Children's Oncology Group repository. U-87 MG and U251 cells were cultured in Eagle's minimum essential medium (EMEM; Sigma) and DMEM, respectively, supplemented with 10% FBS and 1% penicillin/streptomycin. SJGBM2 cells were cultured in Iscove's modified Dulbecco's medium supplemented with 20% of FBS, 5 μg Insulin, 5 μg Transferrin, and 5 ng Sodium Selenite. All cells were maintained at 37°C in 5% CO_2. Cell proliferation and viability were measured using trypan blue exclusion assay. Cell numbers were quantified using a TC100 Automated Cell Counter (BioRad).

Human Primary Cell Harvest and Culture

Resected tumors were collected at the Henry Ford Hospital, with written consent from patients in accordance with institutional guidelines as approved by the Institutional Review Board at Henry Ford Hospital. Pathology was graded according to the WHO criteria. The cells were extracted and cultured as spheres as described previously (deCarvalho et al., 2010).

Cell Sorting

Cells were incubated for 48 hr in stem cell media. Pellets were resuspended in PBS buffer (pH 7.4) containing 0.1% BSA, (B1). Magnetic beads (Dynabeads M-450 Epoxy, Invitrogen) labeled with CD133 antibody were incubated with 2.5×10^6 cells in 1 ml B1 solution. Suspension was incubated 20 min at 4°C with gentle rotation followed by 2 min positive isolation using EasySep magnet (Stem Cell Technologies, #18000). Bead-bound cells were washed 4 times using 1 ml PSB buffer.

Cell Pair Assay and Immunofluorescence

Single cells were isolated with 0.05% Trypsin-EDTA and plated in a drop of media onto MaxGel ECM-coated (Sigma, E0282) coverslips. Cell division was monitored over 20 hr and then fixed in 3.7% paraformaldehyde (PFA) for 20 min at room temperature. Cells were washed, permeabilized, and incubated with 1:200 Numb antibody (Cell Signaling, C29G11). Alexa-488 conjugated secondary antibody (1:1,000 dilution) (Invitrogen) was applied for 1/2 hr. Nuclei were stained with TOTO-3 T-3600 (Molecular Probes). CD133 antibody (Abcam, 27699) staining was performed directly in media without fixation and was followed by the immunofluorescence protocol. Five random fields of view were scored for Numb protein distribution in mitotic cell pairs/treatment/replicate. Primary brain tumor cells were incubated with CDK2 inhibitor NU2058 at the concentration of 30 μM in media for 48 hr. Analysis was performed using Leica CTR 6500 microscope (Leica Microsystems) and AF software.

Statistical Analysis

Student's t test was used, and a p value of 0.05 was considered significant. All data are reported as means ± SD. qRT-PCR statistics were performed as described previously (Yuan et al., 2006). Briefly, the Ct value of the housekeeping gene (GAPDH) was subtracted from the corresponding Ct value of a target gene, producing the dCt value that was further subjected to the Student's t test analysis. Statistical analyses and normality testing were performed using Statistica software.

SUPPLEMENTAL INFORMATION

Supplemental Information includes Supplemental Experimental Procedures and five figures and can be found with this article online at http://dx.doi.org/10.1016/j.ccr.2013.12.006.

ACKNOWLEDGMENTS

We thank Drs. L. Chen, D. Donoghue, and B. Welm for cells and plasmids, J. Ritchie and A. Malysa for statistical analysis, and J. Maimaiti, K. Matthews, and R. Hepburn for technical assistance. We thank the Brain Tumor Tissue Bank and its funding agency, the Brain Tumor Foundation of Canada, for their donation of brain tumor tissue for this study. We also thank the Light Research Program at the Hermelin Brain Tumor Center for funding the derivation of primary cell lines. L.A.P. acknowledges support from Assumption University and the CIHR New Investigator Program. This study was funded by the Cancer Research Society and the Canadian Cancer Society/Canadian Breast Cancer Research Alliance (#02051).

Received: August 26, 2012
Revised: May 17, 2013
Accepted: December 13, 2013
Published: January 13, 2014

REFERENCES

Al Sorkhy, M., Ferraiuolo, R.M., Jalili, E., Malysa, A., Fratiloiu, A.R., Sloane, B.F., and Porter, L.A. (2012). The cyclin-like protein Spy1/RINGO promotes mammary transformation and is elevated in human breast cancer. BMC Cancer *12*, 45.

Artegiani, B., Lange, C., and Calegari, F. (2012). Expansion of embryonic and adult neural stem cells by in utero electroporation or viral stereotaxic injection. J. Vis. Exp. (68), pii: 4093.

Arumugam, K., MacNicol, M.C., Wang, Y., Cragle, C.E., Tackett, A.J., Hardy, L.L., and MacNicol, A.M. (2012). Ringo/cyclin-dependent kinase and mitogen-activated protein kinase signaling pathways regulate the activity of the cell fate determinant Musashi to promote cell cycle re-entry in Xenopus oocytes. J. Biol. Chem. *287*, 10639–10649.

Bao, S., Wu, Q., Sathornsumetee, S., Hao, Y., Li, Z., Hjelmeland, A.B., Shi, Q., McLendon, R.E., Bigner, D.D., and Rich, J.N. (2006). Stem cell-like glioma cells promote tumor angiogenesis through vascular endothelial growth factor. Cancer Res. *66*, 7843–7848.

Boman, B.M., Wicha, M.S., Fields, J.Z., and Runquist, O.A. (2007). Symmetric division of cancer stem cells—a key mechanism in tumor growth that should be targeted in future therapeutic approaches. Clin. Pharmacol. Ther. *81*, 893–898.

Calegari, F., and Huttner, W.B. (2003). An inhibition of cyclin-dependent kinases that lengthens, but does not arrest, neuroepithelial cell cycle induces premature neurogenesis. J. Cell Sci. *116*, 4947–4955.

Chen, R., Nishimura, M.C., Bumbaca, S.M., Kharbanda, S., Forrest, W.F., Kasman, I.M., Greve, J.M., Soriano, R.H., Gilmour, L.L., Rivers, C.S., et al. (2010). A hierarchy of self-renewing tumor-initiating cell types in glioblastoma. Cancer Cell *17*, 362–375.

Chen, J., McKay, R.M., and Parada, L.F. (2012). Malignant glioma: lessons from genomics, mouse models, and stem cells. Cell *149*, 36–47.

Cheng, A., Gerry, S., Kaldis, P., and Solomon, M.J. (2005a). Biochemical characterization of Cdk2-Speedy/Ringo A2. BMC Biochem. *6*, 19.

Cheng, A., Xiong, W., Ferrell, J.E., Jr., and Solomon, M.J. (2005b). Identification and comparative analysis of multiple mammalian Speedy/Ringo proteins. Cell Cycle *4*, 155–165.

Couturier, L., Vodovar, N., and Schweisguth, F. (2012). Endocytosis by Numb breaks Notch symmetry at cytokinesis. Nat. Cell Biol. *14*, 131–139.

Dean, M., Fojo, T., and Bates, S. (2005). Tumour stem cells and drug resistance. Nat. Rev. Cancer *5*, 275–284.

deCarvalho, A.C., Nelson, K., Lemke, N., Lehman, N.L., Arbab, A.S., Kalkanis, S., and Mikkelsen, T. (2010). Gliosarcoma stem cells undergo glial and mesenchymal differentiation in vivo. Stem Cells *28*, 181–190.

Dehay, C., and Kennedy, H. (2007). Cell-cycle control and cortical development. Nat. Rev. Neurosci. *8*, 438–450.

Di Marcotullio, L., Ferretti, E., Greco, A., De Smaele, E., Po, A., Sico, M.A., Alimandi, M., Giannini, G., Maroder, M., Screpanti, I., and Gulino, A. (2006). Numb is a suppressor of Hedgehog signalling and targets Gli1 for Itch-dependent ubiquitination. Nat. Cell Biol. *8*, 1415–1423.

Dobashi, Y., Kudoh, T., Matsumine, A., Toyoshima, K., and Akiyama, T. (1995). Constitutive overexpression of CDK2 inhibits neuronal differentiation of rat pheochromocytoma PC12 cells. J. Biol. Chem. *270*, 23031–23037.

Dobashi, Y., Shoji, M., Kitagawa, M., Noguchi, T., and Kameya, T. (2000). Simultaneous suppression of cdc2 and cdk2 activities induces neuronal differentiation of PC12 cells. J. Biol. Chem. *275*, 12572–12580.

Donovan, L.K., Potter, N.E., Warr, T., and Pilkington, G.J. (2012). A prominin-1-rich pediatric glioblastoma: biologic behavior is determined by oxygen tension-modulated CD133 expression but not accompanied by underlying molecular profiles. Transl. Oncol. *5*, 141–154.

Durand, B., Fero, M.L., Roberts, J.M., and Raff, M.C. (1998). p27Kip1 alters the response of cells to mitogen and is part of a cell-intrinsic timer that arrests the cell cycle and initiates differentiation. Curr. Biol. *8*, 431–440.

Fiano, V., Ghimenti, C., and Schiffer, D. (2003). Expression of cyclins, cyclin-dependent kinases and cyclin-dependent kinase inhibitors in oligodendrogliomas in humans. Neurosci. Lett. *347*, 111–115.

Fischer, P.M., and Lane, D.P. (2000). Inhibitors of cyclin-dependent kinases as anti-cancer therapeutics. Curr. Med. Chem. *7*, 1213–1245.

Golipour, A., Myers, D., Seagroves, T., Murphy, D., Evan, G.I., Donoghue, D.J., Moorehead, R.A., and Porter, L.A. (2008). The Spy1/RINGO family represents a novel mechanism regulating mammary growth and tumorigenesis. Cancer Res. *68*, 3591–3600.

Gönczy, P. (2008). Mechanisms of asymmetric cell division: flies and worms pave the way. Nat. Rev. Mol. Cell Biol. *9*, 355–366.

Götz, M., and Huttner, W.B. (2005). The cell biology of neurogenesis. Nat. Rev. Mol. Cell Biol. *6*, 777–788.

Guryanova, O.A., Wu, Q., Cheng, L., Lathia, J.D., Huang, Z., Yang, J., MacSwords, J., Eyler, C.E., McLendon, R.E., Heddleston, J.M., et al. (2011). Nonreceptor tyrosine kinase BMX maintains self-renewal and tumorigenic potential of glioblastoma stem cells by activating STAT3. Cancer Cell *19*, 498–511.

Hemmati, H.D., Nakano, I., Lazareff, J.A., Masterman-Smith, M., Geschwind, D.H., Bronner-Fraser, M., and Kornblum, H.I. (2003). Cancerous stem cells can arise from pediatric brain tumors. Proc. Natl. Acad. Sci. USA *100*, 15178–15183.

Hidaka, T., Hama, S., Shrestha, P., Saito, T., Kajiwara, Y., Yamasaki, F., Sugiyama, K., and Kurisu, K. (2009). The combination of low cytoplasmic and high nuclear expression of p27 predicts a better prognosis in high-grade astrocytoma. Anticancer Res. *29*, 597–603.

Hindley, C., and Philpott, A. (2012). Co-ordination of cell cycle and differentiation in the developing nervous system. Biochem. J. *444*, 375–382.

Huang, Y., Liu, Y., Chen, Y., Yu, X., Yang, J., Lu, M., Lu, Q., Ke, Q., Shen, A., and Yan, M. (2009). Peripheral nerve lesion induces an up-regulation of Spy1 in rat spinal cord. Cell. Mol. Neurobiol. *29*, 403–411.

Imai, T., Tokunaga, A., Yoshida, T., Hashimoto, M., Mikoshiba, K., Weinmaster, G., Nakafuku, M., and Okano, H. (2001). The neural RNA-binding protein Musashi1 translationally regulates mammalian numb gene expression by interacting with its mRNA. Mol. Cell. Biol. *21*, 3888–3900.

Jablonska, B., Aguirre, A., Vandenbosch, R., Belachew, S., Berthet, C., Kaldis, P., and Gallo, V. (2007). Cdk2 is critical for proliferation and self-renewal of neural progenitor cells in the adult subventricular zone. J. Cell Biol. *179*, 1231–1245.

Jane, E.P., Premkumar, D.R., and Pollack, I.F. (2006). Coadministration of sorafenib with rottlerin potently inhibits cell proliferation and migration in human malignant glioma cells. J. Pharmacol. Exp. Ther. *319*, 1070–1080.

Jin, F., Gao, C., Zhao, L., Zhang, H., Wang, H.T., Shao, T., Zhang, S.L., Wei, Y.J., Jiang, X.B., Zhou, Y.P., and Zhao, H.Y. (2011). Using CD133 positive U251 glioblastoma stem cells to establish nude mice model of transplanted tumor. Brain Res. *1368*, 82–90.

Kelly, S.E., Di Benedetto, A., Greco, A., Howard, C.M., Sollars, V.E., Primerano, D.A., Valluri, J.V., and Claudio, P.P. (2010). Rapid selection and proliferation of CD133+ cells from cancer cell lines: chemotherapeutic implications. PLoS ONE *5*, e10035.

Kerosuo, L., Piltti, K., Fox, H., Angers-Loustau, A., Häyry, V., Eilers, M., Sariola, H., and Wartiovaara, K. (2008). Myc increases self-renewal in neural progenitor cells through Miz-1. J. Cell Sci. *121*, 3941–3950.

Kippin, T.E., Martens, D.J., and van der Kooy, D. (2005). p21 loss compromises the relative quiescence of forebrain stem cell proliferation leading to exhaustion of their proliferation capacity. Genes Dev. *19*, 756–767.

Knoblich, J.A., Jan, L.Y., and Jan, Y.N. (1995). Asymmetric segregation of Numb and Prospero during cell division. Nature *377*, 624–627.

Korur, S., Huber, R.M., Sivasankaran, B., Petrich, M., Morin, P., Jr., Hemmings, B.A., Merlo, A., and Lino, M.M. (2009). GSK3beta regulates differentiation and growth arrest in glioblastoma. PLoS ONE *4*, e7443.

Kranenburg, O., Scharnhorst, V., Van der Eb, A.J., and Zantema, A. (1995). Inhibition of cyclin-dependent kinase activity triggers neuronal differentiation of mouse neuroblastoma cells. J. Cell Biol. *131*, 227–234.

Lange, C., and Calegari, F. (2010). Cdks and cyclins link G1 length and differentiation of embryonic, neural and hematopoietic stem cells. Cell Cycle *9*, 1893–1900.

Lange, C., Huttner, W.B., and Calegari, F. (2009). Cdk4/cyclinD1 overexpression in neural stem cells shortens G1, delays neurogenesis, and promotes the generation and expansion of basal progenitors. Cell Stem Cell *5*, 320–331.

Lathia, J.D., Gallagher, J., Heddleston, J.M., Wang, J., Eyler, C.E., Macswords, J., Wu, Q., Vasanji, A., McLendon, R.E., Hjelmeland, A.B., and Rich, J.N. (2010). Integrin alpha 6 regulates glioblastoma stem cells. Cell Stem Cell *6*, 421–432.

Lathia, J.D., Hitomi, M., Gallagher, J., Gadani, S.P., Adkins, J., Vasanji, A., Liu, L., Eyler, C.E., Heddleston, J.M., Wu, Q., et al. (2011). Distribution of CD133 reveals glioma stem cells self-renew through symmetric and asymmetric cell divisions. Cell Death Dis. *2*, e200.

Lee, J., Kotliarova, S., Kotliarov, Y., Li, A., Su, Q., Donin, N.M., Pastorino, S., Purow, B.W., Christopher, N., Zhang, W., et al. (2006). Tumor stem cells derived from glioblastomas cultured in bFGF and EGF more closely mirror the phenotype and genotype of primary tumors than do serum-cultured cell lines. Cancer Cell *9*, 391–403.

Lenormand, J.L., Dellinger, R.W., Knudsen, K.E., Subramani, S., and Donoghue, D.J. (1999). Speedy: a novel cell cycle regulator of the G2/M transition. EMBO J. *18*, 1869–1877.

Lu, B., Rothenberg, M., Jan, L.Y., and Jan, Y.N. (1998). Partner of Numb colocalizes with Numb during mitosis and directs Numb asymmetric localization in Drosophila neural and muscle progenitors. Cell *95*, 225–235.

Li, A., Walling, J., Ahn, S., Kotliarov, Y., Su, Q., Quezado, M., Oberholtzer, J.C., Park, J., Zenklusen, J.C., and Fine, H.A. (2009a). Unsupervised analysis of transcriptomic profiles reveals six glioma subtypes. Cancer Res. *69*, 2091–2099.

Li, Z., Wang, H., Eyler, C.E., Hjelmeland, A.B., and Rich, J.N. (2009b). Turning cancer stem cells inside out: an exploration of glioma stem cell signaling pathways. J. Biol. Chem. *284*, 16705–16709.

McAndrew, C.W., Gastwirt, R.F., Meyer, A.N., Porter, L.A., and Donoghue, D.J. (2007). Spy1 enhances phosphorylation and degradation of the cell cycle inhibitor p27. Cell Cycle *6*, 1937–1945.

Middlemas, D.S., Stewart, C.F., Kirstein, M.N., Poquette, C., Friedman, H.S., Houghton, P.J., and Brent, T.P. (2000). Biochemical correlates of temozolomide sensitivity in pediatric solid tumor xenograft models. Clin. Cancer Res. *6*, 998–1007.

Muto, J., Imai, T., Ogawa, D., Nishimoto, Y., Okada, Y., Mabuchi, Y., Kawase, T., Iwanami, A., Mischel, P.S., Saya, H., et al. (2012). RNA-binding protein Musashi1 modulates glioma cell growth through the post-transcriptional regulation of Notch and PI3 kinase/Akt signaling pathways. PLoS ONE *7*, e33431.

Narita, Y., Nagane, M., Mishima, K., Huang, H.J., Furnari, F.B., and Cavenee, W.K. (2002). Mutant epidermal growth factor receptor signaling down-regulates p27 through activation of the phosphatidylinositol 3-kinase/Akt pathway in glioblastomas. Cancer Res. *62*, 6764–6769.

NCI. (2005). caIntegrator. http://rembrandt.nci.nih.gov.

Noseda, M., Chang, L., McLean, G., Grim, J.E., Clurman, B.E., Smith, L.L., and Karsan, A. (2004). Notch activation induces endothelial cell cycle arrest and participates in contact inhibition: role of p21Cip1 repression. Mol. Cell. Biol. *24*, 8813–8822.

Pacey, L.K.K., Stead, S., Gleave, J.A., Tomczyk, K., and Doering, L.C. (2006). Neural stem cell culture: Neurosphere generation, immunocytochemical analysis and cryopreservation. Nat. Protoc. *1*, 215–222.

Porter, L.A., Dellinger, R.W., Tynan, J.A., Barnes, E.A., Kong, M., Lenormand, J.L., and Donoghue, D.J. (2002). Human Speedy: a novel cell cycle regulator that enhances proliferation through activation of Cdk2. J. Cell Biol. *157*, 357–366.

Porter, L.A., Kong-Beltran, M., and Donoghue, D.J. (2003). Spy1 interacts with p27Kip1 to allow G1/S progression. Mol. Biol. Cell *14*, 3664–3674.

Reynolds, B.A., and Weiss, S. (1992). Generation of neurons and astrocytes from isolated cells of the adult mammalian central nervous system. Science *255*, 1707–1710.

Sakakibara, S., Nakamura, Y., Yoshida, T., Shibata, S., Koike, M., Takano, H., Ueda, S., Uchiyama, Y., Noda, T., and Okano, H. (2002). RNA-binding protein Musashi family: roles for CNS stem cells and a subpopulation of ependymal cells revealed by targeted disruption and antisense ablation. Proc. Natl. Acad. Sci. USA *99*, 15194–15199.

Sasaki, K., Tamura, S., Tachibana, H., Sugita, M., Gao, Y., Furuyama, J., Kakishita, E., Sakai, T., Tamaoki, T., and Hashimoto-Tamaoki, T. (2000). Expression and role of p27(kip1) in neuronal differentiation of embryonal carcinoma cells. Brain Res. Mol. Brain Res. *77*, 209–221.

Sell, S. (2005). Leukemia: stem cells, maturation arrest, and differentiation therapy. Stem Cell Rev. *1*, 197–205.

Singh, S.K., Hawkins, C., Clarke, I.D., Squire, J.A., Bayani, J., Hide, T., Henkelman, R.M., Cusimano, M.D., and Dirks, P.B. (2004). Identification of human brain tumour initiating cells. Nature *432*, 396–401.

Song, Y., and Lu, B. (2012). Interaction of Notch signaling modulator Numb with α-Adaptin regulates endocytosis of Notch pathway components and cell fate determination of neural stem cells. J. Biol. Chem. *287*, 17716–17728.

Stone, A., Sutherland, R.L., and Musgrove, E.A. (2012). Inhibitors of cell cycle kinases: recent advances and future prospects as cancer therapeutics. Crit. Rev. Oncog. *17*, 175–198.

Venugopal, C., Li, N., Wang, X., Manoranjan, B., Hawkins, C., Gunnarsson, T., Hollenberg, R., Klurfan, P., Murty, N., Kwiecien, J., et al. (2012). Bmi1 marks intermediate precursors during differentiation of human brain tumor initiating cells. Stem Cell Res. (Amst.) *8*, 141–153.

Verhaak, R.G., Hoadley, K.A., Purdom, E., Wang, V., Qi, Y., Wilkerson, M.D., Miller, C.R., Ding, L., Golub, T., Mesirov, J.P., et al.; Cancer Genome Atlas Research Network (2010). Integrated genomic analysis identifies clinically relevant subtypes of glioblastoma characterized by abnormalities in PDGFRA, IDH1, EGFR, and NF1. Cancer Cell *17*, 98–110.

Wang, J., Wang, H., Li, Z., Wu, Q., Lathia, J.D., McLendon, R.E., Hjelmeland, A.B., and Rich, J.N. (2008). c-Myc is required for maintenance of glioma cancer stem cells. PLoS ONE *3*, e3769.

Yan, X., Ma, L., Yi, D., Yoon, J.G., Diercks, A., Foltz, G., Price, N.D., Hood, L.E., and Tian, Q. (2011). A CD133-related gene expression signature identifies an aggressive glioblastoma subtype with excessive mutations. Proc. Natl. Acad. Sci. USA *108*, 1591–1596.

Yoon, C.H., Kim, M.J., Kim, R.K., Lim, E.J., Choi, K.S., An, S., Hwang, S.G., Kang, S.G., Suh, Y., Park, M.J., and Lee, S.J. (2012). c-Jun N-terminal kinase has a pivotal role in the maintenance of self-renewal and tumorigenicity in glioma stem-like cells. Oncogene *31*, 4655–4666.

Yuan, J.S., Reed, A., Chen, F., and Stewart, C.N., Jr. (2006). Statistical analysis of real-time PCR data. BMC Bioinformatics *7*, 85.

Zeppernick, F., Ahmadi, R., Campos, B., Dictus, C., Helmke, B.M., Becker, N., Lichter, P., Unterberg, A., Radlwimmer, B., and Herold-Mende, C.C. (2008). Stem cell marker CD133 affects clinical outcome in glioma patients. Clin. Cancer Res. *14*, 123–129.

Zhang, L., Shen, A., Ke, Q., Zhao, W., Yan, M., and Cheng, C. (2012). Spy1 is frequently overexpressed in malignant gliomas and critically regulates the proliferation of glioma cells. J. Mol. Neurosci. *47*, 485–494.